SSRG International Journal of Electrical and Electronics Engineering
ISSN: 2348-8379/ https://doi.org/10.14445/23488379/IJEEE-V12I1P104
Volume 12 Issue 1, 25-31, January 2025

Original Article

Voltage and Frequency Stability Enhancement with an Automatic Voltage Regulator and Power System Stabilizer in a Ring-Structured Power System Post Generator Loss

Zetty Adibah Kamaruzzaman[1*], Nur Zahirah Mohd Ali[1], Ahmad Syahiman Mohd Shah[1]

[1]*Faculty of Electrical and Electronics Engineering Technology, Universiti Malaysia Pahang Al-Sultan Abdullah, Malaysia.*

[*]*Corresponding Author : zettyadibah@umpsa.edu.my*

Received: 03 November 2024 Revised: 05 December 2024 Accepted: 06 January 2025 Published: 25 January 2025

***Abstract** - Generator loss resulting from failures and inadequate circuit breaker response time can lead to uncontrolled oscillations and possibly system instability. This issue becomes increasingly evident in systems that are small and interdependent among their components. Thus, it is critical to understand the system's transient behavior during generator loss and the important control methods to mitigate the negative impacts. This study analyses the transient stability of the IEEE 9-bus test system in the context of generator loss and delayed circuit breaker response, emphasizing the impact of Automatic Voltage Regulator (AVR) and Power System Stabilizer (PSS) on damping reduction and transient recovery time. The simulation demonstrates that it is essential to clear the faults by opening the circuit breaker before the Critical Clearing Time (CCT) to maintain system stability. Incorporating AVR and optimizing PSS tuning contributes to less damping and accelerating transient recovery time. This allows the voltage dip and prolonged frequency oscillation to recover within the timeframes recommended by IEEE 1159 and IEEE 1547.*

***Keywords** - Generator loss, Uncontrolled oscillations, Voltage dip, Critical clearing time, Transient recovery time.*

1. Introduction

Disturbances such as generator loss can damage grid components and negatively affect the stability of a system. During severe faults, circuit breakers provide over-current protection, but insufficient time response may lead to unnecessarily disconnecting generators. This abrupt disconnection can cause uncontrolled oscillations on the generator's rotor angle, leading to system-wide issues, such as voltage collapse, if not managed properly. The stability of the rated voltage is directly influenced by the reactive power equilibrium of the power system. Thus, understanding the system's behaviour during a generator loss is essential to maintaining system reliability and resilience. Excitation systems and Automatic Voltage Regulators (AVRs) are common and the most outstanding control measures for mitigating the adverse consequences of power system disturbances [1, 2]. AVRs are closed-loop systems that regulate the terminal voltage of synchronous generators in power facilities, ensuring reactive power equilibrium. AVRs and exciters work together to maintain stable voltage levels during disturbances and reduce system-wide instability by maintaining synchronism between generators and dampening oscillations. IEEE 421.5TM-2016 standard specifies the most realistic AVR model with a restricted controller and an exciter while considering the saturation factor [3]. The AVRs and Power System Stabilizer (PSS) work together to maintain stable voltage levels to reduce system-wide instability.

PSS is an established technology that dampens electro-mechanical oscillations via a synchronous machine Excitation Control System (ECS) by cascading the PSS with an AVR [4]. The PSS control parameters need to be adequately designed to provide damping over a range of different conditions to mitigate the potential for prolonged oscillations, which could otherwise result in instability [5-7]. This study examines the transient stability of the IEEE 9-bus test system due to generator loss during a severe fault and delayed circuit breaker time response. The test system's ring circuit topology increases interdependence, as disturbances can spread to the network, causing cascaded voltage drops and oscillations. The goal is to examine the effects of the exciter, AVR, and PSS on damping reduction and the acceleration of transient recovery times in a small, interdependent system. The proposed system configuration and fine-tuning of AVR and PSS in this study enable the system to operate in accordance with EEE 1159 and IEEE 1547, which is practical for the power system industry.

2. Problem Formulation of Transient Stability

For a given initial operating condition, an electrical power system can be classified as stable if the system can regain a state of operating equilibrium after being subjected to a physical disturbance, with most system variables bounded so that practically the entire system remains intact [8, 9]. The electrically generated power is described by Equation (2), and at steady state, when the power loss is zero, the electrical power P_e equals the mechanical power

$$P_m \ (P_e = P_m) \tag{1}$$

$$P_e = \frac{|E||V|}{X} \sin \delta \tag{2}$$

Where E is the constant voltage behind the synchronous reactance in p.u., V is the infinite bus load voltage in p.u., and X is the steady state reactance between the generator and the bus. Transient stability studies examine the impact of significant disturbances such as faults, generation loss, or abrupt load changes. During these disturbances, the rotor will decelerate or accelerate relative to the synchronously rotating air gap, resulting in relative motion. This relative motion is defined by the swing equation, represented in Equation (3).

$$\frac{2\,H}{\omega_o} \frac{d^2\delta}{dt^2} = P_m - P_{max} \sin \delta \tag{3}$$

Where P_m is the mechanical power input in p.u., P_{max} is the maximum electrical power output in p.u., H is the inertia constant, and δ is the rotor angle in electrical radians. Equation (3) is frequently expressed in terms of frequency, f_o where,

$$\frac{2\,H}{\pi f_o} \frac{d^2\delta}{dt^2} = P_m - P_e \tag{4}$$

In a power system with multiple synchronous generators, the simplified two-machine transient stability analysis relies on certain assumptions, including the constant state of generator excitation voltages during fault and post-fault conditions. The swing equation, neglecting damping, is expressed by Equation (5).

$$\frac{H_i}{\pi f_o} \frac{d^2\delta_i}{dt^2} = P_{mi} - \sum_{j=1}^{m} |E_i^{`}||E_j^{`}| \, |X_{ij}| \cos(\theta_{ij} - \delta_i + \delta_j) \tag{5}$$

where Y_{ij} is the elements of the faulted reduced bus admittance matrix, and H_i is the inertia constant of machine i in seconds. The transient stability of a test system can be assessed using the solution of Equation (5). During significant disturbances, an imbalance between mechanical and electrical power occurs, resulting in the prime mover accelerating and the rotor angle increasing. If the steady-state maximum power angle (0°<δ<90°) or the transient swing rotor angle (-180°<δ<180°) surpasses their threshold, beyond which the controllers' actions are ineffective, the power system will lose synchronism [8]. At $\delta = \pm 180°$, the internal voltage angle will be out of phase with the reference voltage, resulting in a substantial current in the generator loop. The generator's current and voltage will oscillate in accordance with variations in rotor angle. Excessive voltage and current levels in oscillatory mode might damage equipment or cause the generator to trip. Nonetheless, for stability and economic considerations, the power system predominantly functions at a power angle between 30° and 45°.

3. Test System Description

The IEEE 9-bus test system, seen in Figure 1, is a transmission network comprising three generators, nine buses, and three loads. The generators are connected at base voltage levels of 13.8 kV, 16.5 kV, and 18 kV. All three loads connect at 230 kV busses. Generator G1 functions as a slack bus, equilibrating the active and reactive power within the entire system. The active and reactive power injected by G1 is determined using Equations (6) and (7).

$$P_{G1} = P_{total\ load} + P_{losses} - P_{G2} - P_{G3} \tag{6}$$

$$Q_{G1} = Q_{total\ load} + Q_{losses} - Q_{G2} - Q_{G3} \tag{7}$$

The synchronous generators and loads are dynamically modelled for transient stability assessments. Tables 1 and 2 present the dynamic data for the loads and generators, respectively. Understanding technical specifications is essential for safety and security, as grid codes vary between nations. In the event of abrupt and significant disturbances, the voltage may transiently collapse to zero until the fault is cleared. The system should stabilize by returning to its equilibrium condition and operating within the ± 10% nominal voltage and ± 5% nominal frequency operational limits.

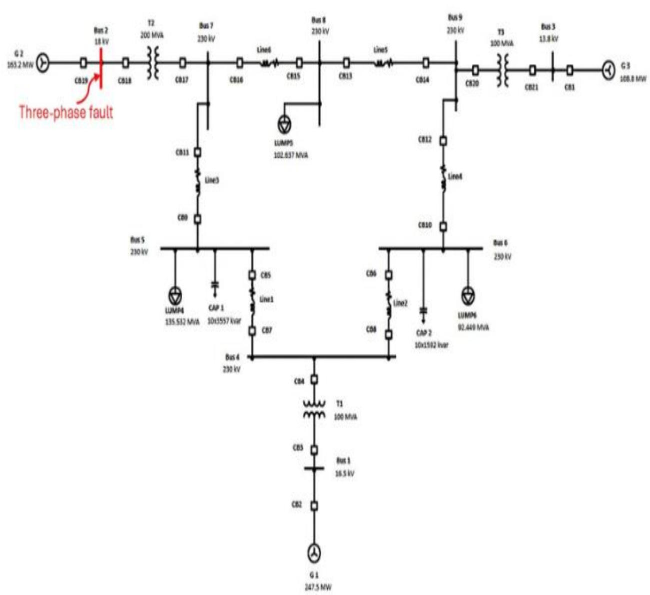

Fig. 1 Modified (data) IEEE 9-bus test system

Table 1. Dynamic load data

Parameters	Load A	Load B	Load C
Model type	Conventional		
Load type	80% Motor, 20% Static		
Rated Power (MVA)	135.532	92.449	102.637
Rated voltage (kV)	230		
Power factor (%)	85		

Table 2. Dynamic generator data

Parameters	G1	G2	G3
Type	Steam Turbo		
Rotor	Salient-Pole	Round-Rotor	Round-Rotor
Rated power (MVA)	247.5	192	128
Rated voltage (kV)	16.5	18	13.8
Power factor (%)	100	85	85
No. of poles	40	2	2
H (MW-sec/MVA)	28.65	29.97	21.15
Damping	5	5	5
Xd (%)	36.135	211	211
Xdu (%)	36.413	211	211
Xd' (%)	15.048	23	23
Xq (%)	15.05	201	201
Xqu (%)	15.117	201	201
Xq' (%)	N/A	46	46
Xq" (%)	N/A	12	12
X_L (%)	8.316	13	13
Tdo' (s)	8.96	6.8	6.8
Tdo" (s)	N/A	0.04	0.04
Tqo' (s)	N/A	0.59	0.59
Tqo" (s)	N/A	0.08	0.08

All generators in this study used the IEEE AC Exciter Type AC2A excitation systems and AVR models, representing a high initial response mechanism. Two additional field current feedback loops equip the alternator main exciter, which it utilizes in conjunction with non-controlled rectifiers. This study equips the IEEE Type PSS1A model with a transducer that converts the measured signal into a voltage signal.

A configurable lead-lag network phase shifts the PSS output to account for time delays in the generator field and excitation system. The washout module continuously balances the PSS output and prevents it from biasing the generator voltage for protracted frequency or power excursions.

The module amplifies and transmits the resulting signal. The signal limiter reduces the output signal's on-load rejection and maintains the beneficial effect of forcing during disturbances. Table 3 displays the parameters for IEEE AC Exciter Type AC2A and IEEE Type PSS1A.

Table 3. Exciter and PSS data for all generators

Description	Parameters
IEEE AC Exciter Type AC2A	V_{RMAX} = 105, V_{RMIN} = -95, S_{EMAX} = 0.04, $S_{E0.75}$ = 0.01, E_{FD} = 4.4, V_{AMAX} = 8, V_{AMIN} = -8, K_A = 400, K_B = 25, K_C = 0.28, K_D = 0.35, K_E = -1, K_F = 0.03, K_H = K_L = 1, T_A = 0.01, T_B = T_C = 0, T_E = 0.6, T_F = 1, T_R = 0, V_{OEL} = 11
IEEE Type PSS1A	V_{SI} = speed, K_S = 3.15, V_{STMAX} = 0.3, V_{STMIN} = -0.9, A_1 = A_2 = 0, T_1 = T_3 = 0.76, T_2 = T_4 = T_6 = 0.1, T_5 = 1

4. Transient Stability Performance Analysis

This section analyses the transient stability of the test system in the event of generator loss as a result of a three-phase fault. The analysis focuses on three critical aspects: (1) calculating the Critical Clearing Time (CCT) for a fault at the generator bus; (2) examining the system's transient stability in the event of a three-phase fault at Bus 2 with an active protection system; and (3) assessing the role of excitation systems, AVR, and PSS in enhancing system stability.

Bus 2 is selected due to the generator's essential role in supplying the network, which makes it the most susceptible to a fault, which poses the biggest risk to the system's stability.

4.1. Case 1: Determination of Critical Clearing Time (CCT)

The CCT is an ideal duration for eliminating disturbances without compromising system performance; system stability is maintained if disturbances are addressed before this timeframe [10]. At t = 1s, a three-phase fault occurs, followed by its clearing at t = 1.6s. Assuming that the initial level of protection is inoperative, the fault is sustained for 600 ms. In practice, the time required to clear the fault will be substantially shorter. The fault duration is incrementally varied to determine the CTC of the generator bus. Table 4 shows the CTC for G2 and G3, and the simulation result is shown in Figures 2 and 3.

A three-phase fault represents the most critical condition. In the event of a fault, the voltage at the fault location drops to zero, and the fault current exhibits reactive characteristics. In contrast, the voltage at other locations in the system depends upon the relative impedances and the current distribution towards the fault point. Severe voltage drops may result in disconnection of the load or cause rotating loads to draw a significantly higher current. This increased current will heighten the stability issue.

Table 4. Critical clearing time, CTC for G2 and G3

Generator	Critical Clearing Time, CTC
G2 (Operating values: 163 MW, 6.56 MVar)	469 ms
G3 (Operating values: 85 MW, -10.885MVar)	575 ms

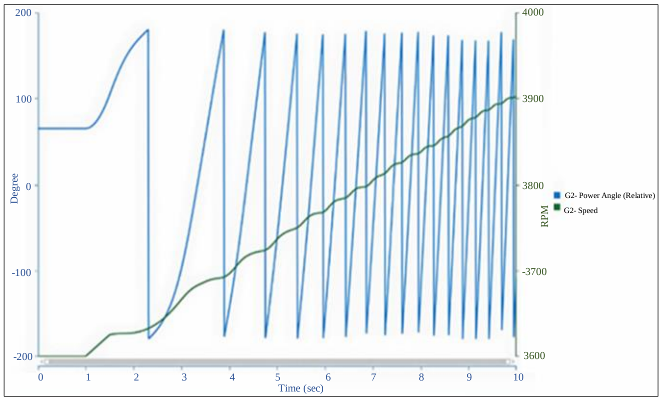

Fig. 2 Transient instability of G2 relative power angle and speed

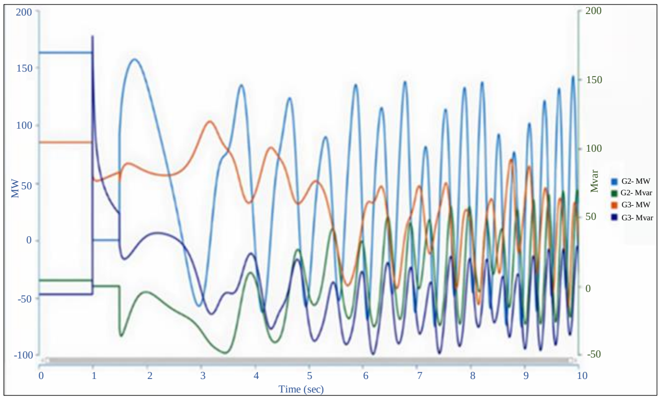

Fig. 3 Transient instability of generators' active and reactive power

Figure 2 illustrates the transients in speed and the relative power angle of the generator, while Figure 3 illustrates the transients in the active and reactive power of the generators. After 300 ms, the generator power angle has already swung, and the speed continues to increase with undulations.

The active and reactive power of the generator fluctuates significantly. The power angle swing exhibits no signs of recovery, indicating system instability. When a generator loses synchronization, it experiences cyclic pressures and torques that affect the machine's foundations, shaft, and mechanical systems.

4.2. Case 2: Generator Loss during Three-Phase Fault

At t = 1s, Bus 2 experiences a three-phase fault. Assuming the problem is temporary, the circuit breakers CB18 and CB19 operate in synchronization, eliminating the fault instantly upon the breaker opening at t = 1.05s. Circuit breakers CB18 and CB19 subsequently close in coordination at t = 1.20s. The three-phase fault is cleared before the CTC, as shown in Table 4.

Figure 4 illustrates the voltage profile for all buses in this case. The G2 connects to Bus 2, supplying a substantial share of the system's active and reactive power. A three-phase fault at this bus induces a critical short circuit, leading to an almost complete voltage drop to 0% of the nominal voltage. The equilibrium between supply and demand is temporarily disrupted.

The largest generator encounters difficulties sustaining synchronization with the grid during and after the fault, leading to oscillations across the system. The problem sustains for 50 ms, and the voltage drop at Bus 2 disseminates throughout the entire system, resulting in a cascading impact.

The 9-bus test system's configuration, defined by the interconnection of buses and power flow through various transmission lines in loops, resembles a ring circuit topology. This structure makes the system more dependent on each other, which means that a problem at Bus 2 can easily spread through the network, causing the same voltage drops and oscillations all over the system, as shown in Figure 4.

At t = 1.05 s, the circuit breaker activates, eliminating the fault. After the fault clearance, the voltage at all buses starts oscillating as the system attempts to stabilize. These oscillations indicate underdamped behaviour, signifying that the system is undergoing low-frequency oscillations.

According to IEEE 1159, the post-fault voltage shows a reduction exceeding 10% from the nominal voltage for approximately 1s, indicating a momentary voltage sag. Thus, in sensitive industrial or commercial environments where power quality is crucial, the system requires additional voltage support to comply with IEEE 1159's power quality requirement.

Figure 6 illustrates a sudden shift in active and reactive power for both generators starting at the fault point (t = 1s) and beginning to stabilize after t = 3s. G2 temporarily disconnects from the system when the circuit breaker opens to clear the fault, resulting in a reduction in power generation.

After closing the circuit breaker (t = 1.20s), G2 resumes its operation and may incrementally increase its active power to reestablish equilibrium and address inadequate load demands during the fault.Concurrently, G3 mitigates the situation by providing more reactive power to the system during the fault while the generator's internal Electromotive Force (EMF) attempts to offset the voltage drop.

This reaction is influenced by the intrinsic properties of the generator's excitation mechanism, which is designed to sustain internal voltage despite external perturbations. The surge at the fault location naturally stabilizes the voltage at other buses by providing additional reactive power to meet the reactive load demand.

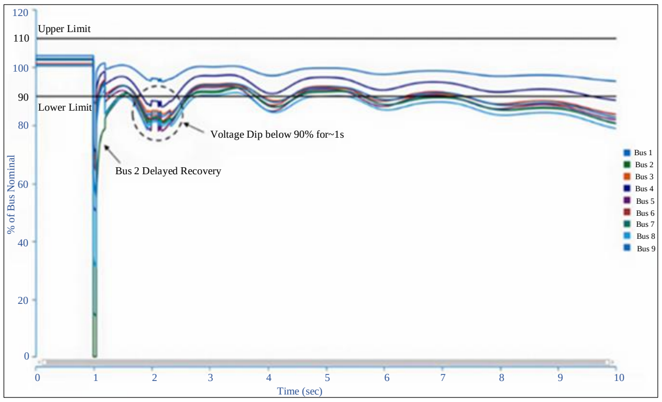

Fig. 4 Transient voltage of all buses during G2 loss

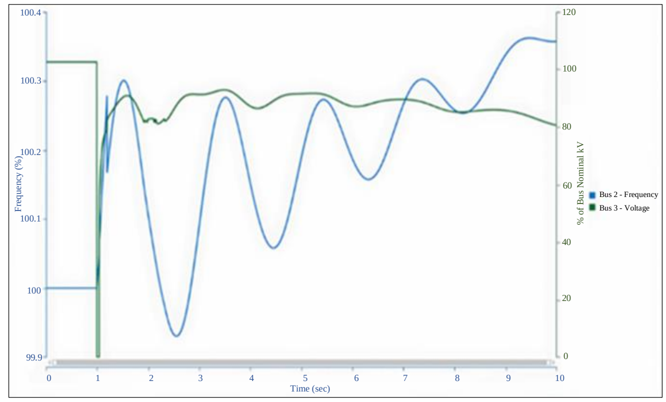

Fig. 5 Transient voltage and frequency of bus 2 during G2 loss

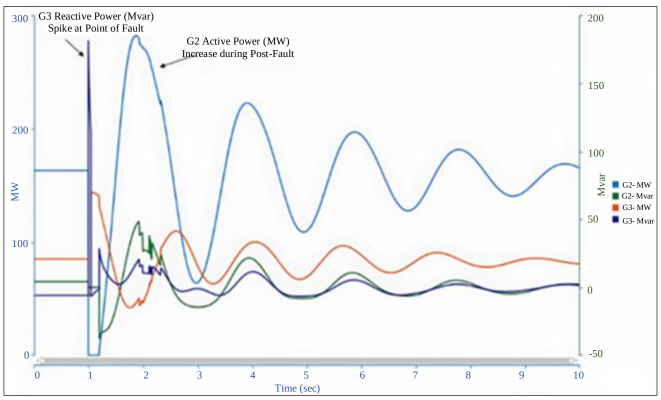

Fig. 6 Abrupt changes in generators active and reactive power during G2 loss

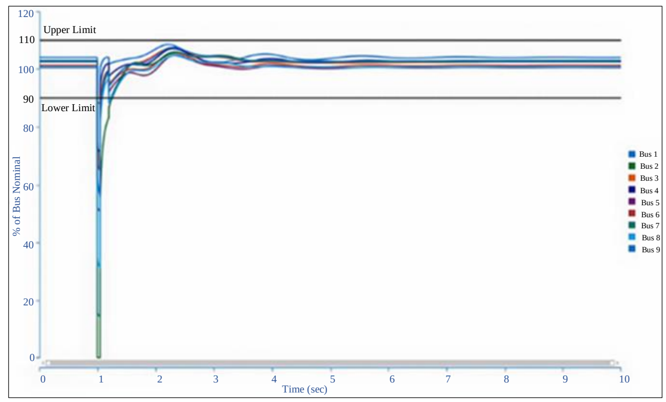

Fig. 7 Transient voltage improvement with exciter and PSS

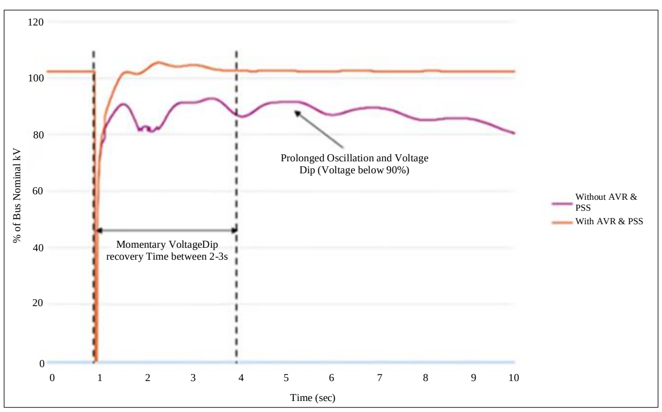

Fig. 8 Comparison between transient voltage recovery at bus 2

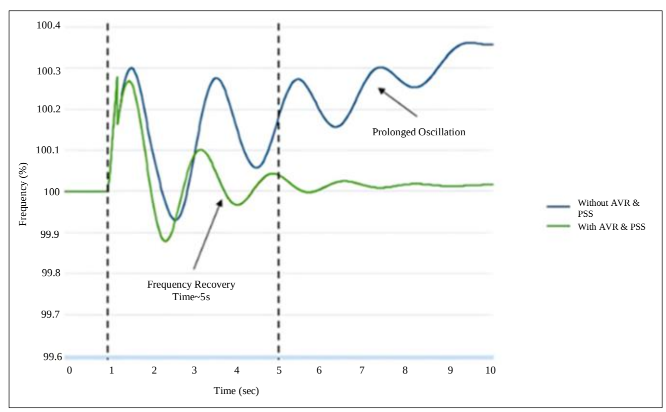

Fig. 9 Comparison between transient frequency recovery at bus 2

4.3. Case 3: Improving Post-Fault System Stability

The findings in Case 2 show that the lack of control mechanisms intensifies the system's response to instability. The generator's internal dynamics and the field winding's response intensify this behaviour, especially when no AVR or PSS is in place to regulate and mitigate the voltage and power post-fault. In this case, excitation systems, an AVR, and a PSS are configured to stabilize the system during the transient recovery period. The recovery duration is essential for evaluating system stability since prolonged oscillations in voltage or frequency can affect equipment and operational reliability. Figures 7, 8, and 9 illustrate a marked improvement in transient stability following faults due to the addition of AVR and PSS.

The AVR adjusts the generator excitation in response to the terminal voltage. The system produces more reactive power to counteract the dip effects when the generator terminal voltage decreases. Simultaneously, the PSS counteracts low-frequency oscillations, thereby mitigating rotor angle and speed oscillations and enhancing system stability.

Optimal tuning of PSS helps suppress the damping and shorten the transient recovery time, as shown in Figure 7. Figure 8 demonstrates that the installation of AVR and PSS allows the momentary voltage dip following faults to recover within 3s, thereby preventing prolonged low-voltage conditions for the connected loads. Similarly, Figure 9 demonstrates that the installation of AVR and PSS resolves the issues with generation-load balance and insufficient system inertia, as the frequency at Bus 2 recovers within 5s. IEEE 1159 and IEEE 1547 provide voltage dip and frequency recovery time guidelines, respectively [11, 12].

5. Conclusion

This study examines the transient effects resulting from losing the largest generator in the IEEE 9-bus test system. A three-phase fault occurs at Bus 2, prompting the relevant circuit breaker to be triggered to clear the fault within the CTC. Upon the disconnection of generator G2 from the system, the voltage at Bus 2 undergoes a total drop to 0% of the nominal voltage and then recovers after the fault is cleared. Nevertheless, the system encountered brief instability during the transitory recovery phase due to the slight delay between the breaker's opening and reclosing. The test system's structure, identical to a ring circuit, results in interdependence among its components.

Consequently, disruptions may propagate through the network, resulting in cascading voltage drops and oscillations. The integration of IEEE AC Exciter Type AC2A and IEEE Type PSS1A across all generators in the system aids in mitigating transient stability issues. This study's recommended system configuration and optimization of AVR and PSS facilitate compliance with EEE 1159 and IEEE 1547, making it applicable to the power system industry.

The simulation demonstrated an enhancement in bus voltage and frequency following the fault, attributed to the incorporation of AVR and PSS. The AVR regulates bus voltage by dynamically modifying generator excitation to mitigate dip effects. Simultaneously, the PSS alleviates rotor angle and speed fluctuations, hence improving voltage stability by countering low-frequency oscillations.

5.1. Future Scope

Future studies may examine the effects of incorporating a large-scale solar power plant into the grid. The solar power system will serve as a supplementary source for the grid in the event of conventional generator failure. The research will examine grid stability when the generator disconnects from the grid due to an outage and is immediately substituted by the solar power system. The system is expected to be impacted during the switching event due to the generation-load imbalance and inadequate system inertia.

Acknowledgements

This research is supported by an internal grant from Universiti Malaysia Pahang Al-Sultan Abdullah (RDU230381). The author wishes to thank the anonymous referees whose comments and suggestions greatly enhanced this paper. A special thanks to the project members and the Faculty of Electrical and Electronics Engineering Technology at Universiti Malaysia Pahang Al-Sultan Abdullah.

References

[1] Haluk Gozde, "Robust 2DOF State-Feedback PI-Controller Based on Meta-Heuristic Optimization for Automatic Voltage Regulation System," *ISA Transactions*, vol. 98, pp. 26-36, 2020. [CrossRef] [Google Scholar] [Publisher Link]

[2] Ömer Türksoy, and Arzu Türksoy, "A Fast and Robust Sliding Mode Controller for Automatic Voltage Regulators in Electrical Power Systems," *Engineering Science and Technology, an International Journal*, vol. 53, 2024. [CrossRef] [Google Scholar] [Publisher Link]

[3] "421.5-2016 - IEEE Recommended Practice for Excitation System Models for Power System Stability Studies," *In IEEE Std*, pp.1-207, 2016. [CrossRef] [Publisher Link]

[4] Yuwa Chompoobutrgool, Luigi Vanfretti, and Mehrdad Ghandhari, "Survey on Power System Stabilizers Control and their Prospective Applications for Power System Damping using Synchrophasor-Based Wide-Area Systems," *European Transactions on Electrical Power*, vol. 21, no. 8, pp. 2098-2111, 2011. [CrossRef] [Google Scholar] [Publisher Link]

[5] Xavier Bombois, and Luigi Vanfretti, "Performance Monitoring and Redesign of Power System Stabilizers Based on System Identification Techniques," *Sustainable Energy, Grids and Networks*, vol. 38, 2024. [CrossRef] [Google Scholar] [Publisher Link]

[6] D. Lauria, "Power Systems Stabilizers Online Tuning Based Upon Parameters Dynamic Estimation," *Sustainable Energy, Grids and Networks*, vol. 39, 2024. [CrossRef] [Google Scholar] [Publisher Link]

[7] Kjetil Obstfelder Uhlen et al., "Wide-Area Power Oscillation Damper Implementation and Testing in the Norwegian Transmission Network," *2012 IEEE Power and Energy Society General Meeting*, San Diego, CA, USA, pp. 1-7, 2012. [CrossRef] [Google Scholar] [Publisher Link]

[8] P. Kundur et al., "Definition and Classification of Power System Stability IEEE/CIGRE Joint Task Force on Stability Terms and Definitions," *IEEE Transactions on Power Systems*, vol. 19, no. 3, pp. 1387-1401, 2004. [CrossRef] [Google Scholar] [Publisher Link]

[9] Hadi Saadat, *Power System Analysis*, Mc Graw Hill, 1999. [Google Scholar]

[10] Nur Ashida Salim et al., "System Transient Stability Due to Various Contingency Using Power World Simulator," *2023 IEEE 3rd International Conference in Power Engineering Applications (ICPEA)*, Putrajaya, Malaysia, pp. 279-284, 2023. [CrossRef] [Google Scholar] [Publisher Link]

[11] "1159-2019 - IEEE Recommended Practice for Monitoring Electric Power Quality," *In IEEE Std*, pp. 1-98, 2019. [CrossRef] [Google Scholar] [Publisher Link]

[12] "1547-2018 - IEEE Standard for Interconnection and Interoperability of Distributed Energy Resources with Associated Electric Power Systems Interfaces," *In IEEE Std*, pp. 1-138, 2018. [CrossRef] [Google Scholar] [Publisher Link]